

Effect of hydrogen content on the light induced defect generation in direct current magnetron reactively sputtered hydrogenated amorphous silicon thin films

Mustafa Pinarbasi^{a)}

IBM Corporation, 5600 Cottle Road, San Jose, California 95193

Mark J. Kushner

Department of Electrical and Computer Engineering and the Coordinated Science Laboratory,
University of Illinois at Urbana-Champaign, Urbana, Illinois 61801

John R. Abeison

Department of Materials Science and Engineering and the Coordinated Science Laboratory,
University of Illinois at Urbana-Champaign, Urbana, Illinois 61801

(Received 14 November 1989; accepted for publication 4 May 1990)

The kinetics of light induced defect generation or the Staebler–Wronski effect have been investigated on device quality hydrogenated amorphous silicon films which were deposited by dc magnetron reactive sputtering. The total hydrogen content (C_H) of the films, which varied from ~ 10 to 28 at. %, had a strong influence on the defect generation. Low C_H (10%–15%) films had a high initial density of defect states (~ 7 to $10 \times 10^{15} \text{ cm}^{-3}$) compared to the high C_H (> 17 at. %) films with a density of $\sim 3 \times 10^{15} \text{ cm}^{-3}$. However, light exposure increased the defect density more slowly on the low C_H films, such that after about 1 h of light exposure their defect density was lower. A high-quality glow discharge produced film was also measured, and behaved similarly to the high C_H sputtered films. The greater stability of the low C_H films was also reflected in a slower decrease of the electron photoconductivity relative to the other samples. For exposure times (t) up to 1000 h, the total density of defect states of the films increases as a power law: the high C_H and glow discharge deposited films follow $t^{0.3}$ and $t^{0.32}$, respectively, whereas the low C_H film shows $t^{0.23}$ at long times. The latter behavior is in sharp contrast with previous reports, and indicates that the degradation does not follow the Stutzmann theory or obeys it with a $100 \times$ smaller susceptibility to degradation.

1. INTRODUCTION

Staebler and Wronski¹ discovered that reversible changes of the electronic properties of glow discharge (GD) produced hydrogenated amorphous silicon (*a*-Si:H) films occur when the films are exposed to light. These changes included a decrease in the photo and dark conductivities of the films. They were attributed to an increase in the density of defect states (DOS) in the band gap which act as recombination centers for photo-excited carriers. The excess defect states were shown to be removable by annealing at temperatures greater than 150 °C for 1–2 h and the as-deposited photoconductivity and dark conductivity were recovered. Since its discovery, the light induced degradation of *a*-Si:H has been referred to as the Staebler–Wronski effect (SWE).

Many previous studies worked towards understanding the reversible changes in the DOS and its effects on electronic properties. Hirabayashi *et al.*,² and Dersch *et al.*,³ suggested that the increase in DOS resulted from an increase in the density of silicon dangling bonds which they measured using electron spin resonance (ESR). Other studies using deep-level transient spectroscopy,⁴ luminescence,⁵ and sub-gap absorption by both photothermal deflection spectroscopy⁶

and constant photocurrent method⁷ showed an increase in the DOS of *a*-Si:H upon light exposure. All of these studies concluded that light exposure of the films creates defect states and that these defects control the electronic properties of the *a*-Si:H films by decreasing carrier lifetimes. The silicon dangling bond is known to be trivalent with the energy of the doubly occupied state usually assumed to be higher than the singly occupied state. However, the configuration, capture cross sections and energy distribution of these defect states are still not clear.⁸ The relationship between DOS and photoconductivity is not unique, and varies between samples.

A number of experiments^{9–13} on Schottky barrier devices and diodes have provided clues to the defect generation kinetics in *a*-Si:H. These studies showed that the creation of the defect states was due to the recombination of the excess carriers, independent of how the carriers were formed, e.g., by illumination or current injection. Results on *p-i-p* devices also suggested that trapping of holes can contribute to the degradation process.¹⁴

Microscopic processes were proposed to explain the creation of metastable defect states in *a*-Si:H. The silicon bond breaking model of Pankove and Berkeyheiser⁵ is widely recognized as being a reasonable explanation for the degradation. According to Dersch *et al.*,³ increase in dangling silicon bond density involves two stages. The first stage is the break-

^{a)}This work was carried out while the author was in the Department of Materials Science and Engineering and the Coordinated Science Laboratory of the University of Illinois at Urbana-Champaign.

ing of weak Si—Si bonds that exist in the strained amorphous silicon network. (These weak bonds may further be weakened by hole trapping;¹⁵ however, the majority of the holes trapped in the weak Si—Si bonds do not lead to bond breaking as measured with ESR.)¹⁶ The second stage is the subsequent isolation of these broken bonds. The isolation may result from the exchange of a hydrogen atom between hydrogen-terminated and a dangling bond site before the newly created broken bonds recombine. This microscopic model is shown in Fig. 1.¹⁵

The effect of impurities on the Staebler–Wronski effect (SWE) has also been studied.¹⁵ Concentrations of oxygen or nitrogen $> 0.1\%$ result in an increase in the magnitude of the SWE. However, films which contain impurities at $\leq 0.1\%$ do not show a dependence of SWE on the concentrations. Based on these results, it has been argued that SWE is an intrinsic property of *a*-Si:H and are not related to the defect states created by the impurities.¹⁵

The degradation kinetics in *a*-Si:H films has been modeled by Stutzmann, Jackson, and Tsai.¹⁵ They assumed that the breaking of weak Si—Si bonds is induced by band to band recombination of free carriers. The model predicts that the density of defect states can be approximated by the following formula:

$$N_s(t) = [A_{s-w} G^2 t + N_s^3(0)]^{1/3}, \quad (1)$$

where $N_s(0)$ is the initial DOS, G is the generation rate ($\text{cm}^{-3} \text{s}^{-1}$) and A_{s-w} is the susceptibility coefficient which is a material constant. There are three key points of the model that should be stressed. The first is that the long-term increase in the DOS is proportional to $t^{1/3}$ and is independent of the initial DOS. The second is that the films with higher initial DOS show a slower relative rate of degradation in the initial stages but the total DOS for these films does not become lower than the films which have lower initial DOS. The third point is that the photoconductivity exponent γ or δ (where $\sigma_{\text{ph}} \propto G^\gamma$ or $\sigma_{\text{ph}} \propto N_s^{-\delta}$) was measured to be near unity¹⁵ and taken to be 1 in the model. These aspects of the model will be discussed in the following sections with respect to the magnetron reactive sputtered *a*-Si:H films.

The effect of hydrogen content and bonding on SWE in glow discharge produced *a*-Si:H have been studied by many groups but the results are contradictory. Shimizu *et al.*¹⁷ have grown *a*-Si:H films with both glow discharge and magnetron sputtering techniques. They reported that the num-

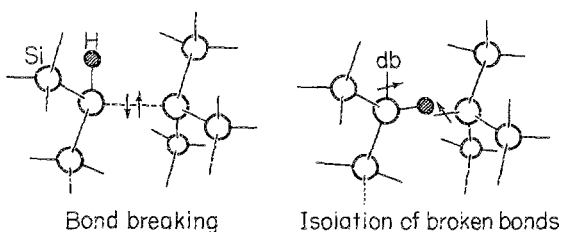


FIG. 1. The two stage microscopic degradation mechanism.¹⁵ The first step is the breaking of weak Si—Si bonds. The second step involves the isolation of these defect states by hydrogen atoms.

ber of defect states created due to light exposure increases as the initial DOS of the films increases, and that the number of additional defect states increases linearly with the hydrogen content. However, the initial DOS of their films was high, ranging from 2×10^{16} to $3 \times 10^{18} \text{ cm}^{-3}$. Ohsawa *et al.*¹⁸ performed measurements on films which contain DOS between 1×10^{16} and $2 \times 10^{17} \text{ cm}^{-3}$ after annealing at 150°C . They found that films with higher initial defect states are more susceptible to SWE. However, if they annealed the films at $300\text{--}450^\circ\text{C}$, the number of created defect states decreased as they increased the annealing temperature for films with higher initial defect density. They found a weak dependence of SWE on C_{H} . The total hydrogen content and bonding configuration of hydrogen was determined from infrared absorption studies. They observed that the degradation properties of their films were independent of the monohydride (SiH) or dihydride (SiH₂) concentrations. However, hydrogen evolution studies showed an increase in susceptibility to SWE for films in which the amount of hydrogen evolved at low temperature increased. Nakano *et al.*¹⁹ at Sanyo laboratories observed a correlation between the SiH₂ concentration and SWE. However, they did not report on the relation between the total hydrogen content and the SiH₂ concentration. They found that light-induced defect states increase as the SiH₂ concentration in the films increased.

Carlson²⁰ developed a model for light-induced degradation that involves the motion of hydrogen on the internal surfaces of microvoids. He proposed that increasing the density of the material should increase the stability of *a*-Si:H. Bhattacharya and Mahan²¹ reported that increasing the microstructure (associated with dihydride density) of *a*-Si:H increases the light induced defect states. This supports the model proposed by Carlson.²⁰

Previous SWE studies have concentrated on glow discharge produced films and there has been no detailed work concerning reactively sputtered (RS) material. Reactive sputtering of *a*-Si:H (Refs. 22–28) has an important experimental advantage over other deposition methods: the hydrogen content (C_{H}) can be independently controlled via the hydrogen partial pressure in the discharge, leaving other deposition parameters such as the substrate temperature fixed. We previously reported that our dc magnetron RS *a*-Si:H films are device quality as judged by the microstructural, optical, electronic properties,^{29,32} internal photoemission,³³ carrier transport,³⁴ and SWE measurements.³⁵ Here we examine the SWE on these magnetron RS films as a function of C_{H} in detail. The main objectives are to (a) determine the stability of our RS films against SWE, (b) compare the degradation kinetics with published results for glow discharge produced *a*-Si:H and the predictions of the band to band recombination model, and (c) determine the relationship between C_{H} and the SWE on RS films.

II. EXPERIMENTAL PROCEDURES

The films were deposited in a UHV type chamber with base pressures of O₂, CO, and H₂O less than 1×10^{-9} , 1×10^{-9} , and 2.5×10^{-9} Torr, respectively.^{32,36} The growth species were generated by a dc planar magnetron sputtering source with a high-purity 5×12 in. Si target. The $E \times B$ field

restricts the bright glow of the plasma to the vicinity of the target, and only a weak positive column plasma interacts with the substrate. At the low working gas pressure (1 mTorr) fast neutral species sputtered or reflected from the target can reach the substrate with little gas phase thermalization. This bombardment suppresses the tendency to form a columnar microstructure.³⁷ A range of fast particle energies and fluxes are needed to promote a dense microstructure, but not create electronic defects, in *a*-Si:H; the atomic-scale kinetics of this process are not quantitatively understood.³⁸

The range of deposition conditions, electronic and carrier transport properties of the films reported in this study are listed in Table I. The deposition rate of the films was between 30 and 220 Å/min which was controlled via discharge current. The C_H and the properties of the films were independent of the deposition rate in the range we studied.³² The argon partial pressure was kept constant at 1 mTorr for all the films and no columnar microstructure was observed. The hydrogen partial pressure was varied from 0.2 to 1.2 mTorr. Secondary ion mass spectroscopy analysis of representative films (performed at the Charles Evans and Associates Laboratories, Redwood City, Ca) showed that the oxygen, carbon, and nitrogen impurity levels are less than 50, 15, and 5 ppm (parts per million), respectively. These impurity levels are comparable to the best reported values¹⁹ for *a*-Si:H films. The argon concentration in the films was less than 0.1 at. %.

These dc magnetron RS films were device quality in the as-deposited state, with optical and electronic properties comparable to glow discharge deposited films.^{29,30,32} The total C_H was varied from ~10 to 28 at. % mainly by adjusting the hydrogen partial pressure in the discharge. The total C_H of the films decreased from ~28 to ~13 at. % as we decreased the hydrogen partial pressure in the discharge from 1.2 to 0.2 mTorr at a constant substrate temperature (T_s) of 230 °C. Most of our studies are done on these films.

TABLE I. The range of deposition conditions and properties of the films that are studied for light induced degradation measurements.

Deposition temperature (°C)	230–300
Hydrogen partial pressure (mT)	0.2–1.2
Argon partial pressure (mT)	1.0
Cathode current (A)	0.25–0.8
Deposition rate (Å/min)	30–220
Thickness (μm)	0.8–2
Hydrogen content (at. %)	~10–28
Optical band gap (eV)	1.62–1.85
Dark conductivity activation energy (eV)	0.7–0.95
Dark conductivity (Ω cm) ⁻¹	3×10^{12} – 2×10^9
AM-1 photo conductivity (Ω cm) ⁻¹	0.9×10^5 – 3×10^5
AM-1 photo/dark conductivity ratio	1×10^4 – 5×10^5
Electron drift mobility (cm ² /V s)	0.5–2
Electron mobility × recombination lifetime (cm ² /V)	1×10^7 – 3×10^7
Electron mobility × trapping lifetime (cm ² /V)	1.3×10^8 – 8×10^9
Hole mobility × recombination lifetime (cm ² /V)	0.8 – 3.0×10^{-8}
Density of midgap states (cm ⁻³)	1×10^{15} – 1×10^{16}

We also made few films at 0.2 mTorr hydrogen partial pressure but at higher T_s (275 and 300 °C). This resulted in a ~2% decrease in C_H . This is reasonable considering that, at low C_H , (films deposited at lower hydrogen partial pressures), most of the hydrogen bonds in thermally stable monohydride (2000 cm⁻¹) sites as evidenced by thermal evolution data.^{30,32} At higher C_H , monohydride (2000 cm⁻¹) concentration of the films tends to saturate and additional hydrogen goes to the thermally less stable 2100 cm⁻¹ (dihydride and clustered monohydride) mode. As a result, T_s becomes important in controlling the total C_H of the films deposited at higher hydrogen partial pressures.³²

Conductivity and DOS measurements were made using co-planar chromium contacts deposited on top of the film and defining a gap of 0.2 cm. The annealed state photoconductivities were measured under the AM-1 (100 mW/cm²) light.^{29,30} The light exposure measurements were performed using only the red portion of the spectrum from an ENH lamp; low and high band pass filters were used to bracket the wavelengths between 620 and 680 nm (1.83 to 2 eV) with a nearly top hat spectrum. This range of photon energies is higher than the Tauc band gap of all the films studied. The films were placed on a water cooled stage to keep the temperature constant at ~30 °C throughout the light exposure experiments. The intensity of the red light used for light exposure was 150 mW/cm² as measured by a pyroelectric radiometer and the areal illumination of the sample was uniform. Most of the films studied had thicknesses between 1 and 1.6 μm to obtain nearly uniform light absorption throughout the films.

We calculated the volume generation rate (G) for RS films using $G = F(1 - R)(1 - \exp \alpha d)/d$ and integrating between 620 and 680 nm; $F(\lambda)$, $R(\lambda)$, $\alpha(\lambda)$, and d are the photon flux (photons/cm²), reflection coefficient, absorption coefficient (cm⁻¹), and sample thickness (cm), respectively. The use of near band-gap light produces a roughly uniform generation rate throughout the sample. For the high C_H films the generation rates for the topmost 0.2 μm are 35%–50% higher than for the bottom 0.2 μm. For the low C_H films, which have higher absorption coefficients, the topmost 0.2 μm has 5–10 times higher generation rates than the bottom 0.2 μm (which is still comparable or higher than the generation rates for the bottom 0.2 μm of high C_H films). This is obviously not “uniform.” However, previous studies have shown that the defect generation rate proceeds as G^2 ; thus the low C_H films should degrade more rapidly since their average G is a factor of ~2 higher than high C_H films,³² whereas in fact they degrade much more slowly.

The films had previously been exposed to light for 30 min. To restore the as-deposited conditions they were annealed under vacuum at 165 °C for 2 h and slowly cooled to room temperature (~2 °C/min). This annealed state was evaluated using 5 s of light exposure to measure the initial photoconductivity. The CPM technique was used to determine the DOS.³⁹ Then the films were exposed to light for 30 min with the photoconductivity monitored continuously. The light exposure was interrupted to measure the DOS. This sequence (light exposure and DOS measurements) was performed to 3 and 15 h of total light exposure. For selected

samples, the measurements were continued to 100, 250, 500, and 1000 h of light exposure.

III. RESULTS AND DISCUSSION

A. Hydrogen content, hydrogen bonding, and microstructure

The effect of total C_H on the hydrogen bonding modes and microstructure of these films has been analyzed in detail.^{30-32,40} The total C_H of the films were measured using both infrared absorption and hydrogen thermal evolution techniques.^{30,40} The integrated absorption centered at 640 cm^{-1} (I_{640}) is directly proportional to the total C_H of the films by the relation $N_{\text{H}} = I_{640} \times A_{640}$ where N_{H} (cm^{-3}) is the total number of bonded hydrogen atoms and A_{640} (cm^{-2}) is the constant of the proportionality (oscillator strength). The constant of proportionality for these films was determined to be $2 \times 10^{19}\text{ cm}^{-2}$ ($\pm 10\%$) by comparing the I_{640} with the hydrogen evolution measurements.⁴⁰ The density of the *a*-Si:H films were taken to be $5 \times 10^{22}\text{ cm}^{-3}$. The integrated absorption of the stretching modes was determined after deconvoluting the absorption into two Gaussians centered around 2000 cm^{-1} and 2100 cm^{-1} . Figure 2 shows the ratio of the I_{2100} (dihydride and clustered monohydride content of the films) to the I_{640} , (I_{2100}/I_{640}), as a function of the total C_H of the films. Figure 2 also indicates the ratio of the atomic concentration of hydrogen ($C_{\text{H},2100}/C_H$) in these modes. The constant of proportionality of $3.3 \times 10^{20}\text{ cm}^{-2}$ was used to calculate the $C_{\text{H},2100}$, which was determined by comparing the low-temperature hydrogen evolution peaks and I_{2100} .^{30,40} The monohydride concentration of the films, $C_{\text{H},2000}$, (the integrated absorption at 2000 cm^{-1}) can be calculated from $C_{\text{H},2000} = C_H - C_{\text{H},2100}$. These results show that the total C_H of the films correlates uniquely with the hydrogen bonding

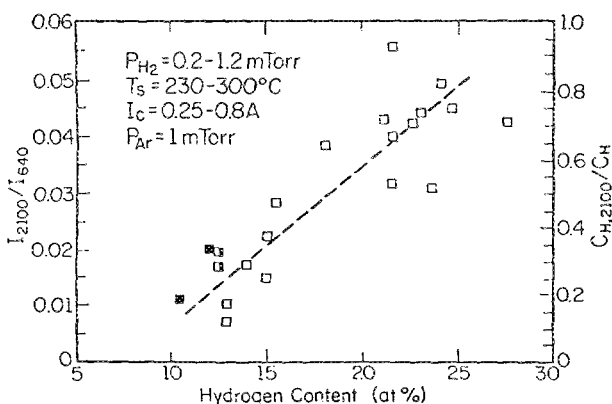


FIG. 2. The ratio of the IR absorption intensity at $I_{2100}\text{ cm}^{-1}$ (the stretching mode of dihydride and clustered monohydride groups) scaled to the absorption intensity at 640 cm^{-1} (the wagging mode, which is proportional to total hydrogen) as a function of C_H . The ratio of the atomic concentrations in these modes is also indicated. The substrate temperature was kept constant at 230°C for all the films, except the filled and half filled data points which were measured on films deposited at 300 and 275°C , respectively: the hydrogen partial pressure during deposition was kept constant at 0.2 Torr for these films.

modes. The low C_H (10–15 at. %) films are monohydride rich. The hydrogen concentration in the 2100 cm^{-1} mode increases nearly linearly as the total C_H of the films increases (Fig. 3) and more than half of the hydrogen is in this mode when C_H exceeds ~ 17 at. %. The films which had 3 and 5 at. % hydrogen had only the 2000 cm^{-1} (monohydride) mode and had poor electronic properties.^{30,40}

Figure 3 shows the hydrogen evolution spectra for two representative (low and high C_H) films. The low C_H film has one hydrogen evolution peak at a high temperature (600°C). In contrast, high C_H film shows three different peaks. A sharp low-temperature peak in the high C_H film indicates a void rich structure.^{30,32} The amount of hydrogen evolved at ~ 375 and 500°C peaks increases nearly linearly as the C_H of the films increases, again indicating that hydrogen bonding modes uniquely correlate with the total C_H of the films.^{30,31} (For a detailed discussion of the subject the reader is referred to references 30, 32, and 40.) In light of these correlations we discuss the SWE of dc magnetron RS films as a function of their total C_H . However, one can analyze the results in terms of hydrogen bonding utilizing Fig. 2 and the correlations given in Refs. 30, 32, and 40.

B. Changes in photoconductivity and dark conductivity

The annealed state photo- and dark conductivities of the magnetron RS films are shown in Fig. 4. All the films used in this study ($10 < C_H < 28$ at. %) had similar σ_{ph} in the as-deposited state under AM-1 (100 mW/cm^2) light. We observed the identical trend in σ_{ph} under 150 mW/cm^2 red light. The films containing C_H greater than 30 at. % are not of high electronic quality in the as-deposited state²⁹ and will not be dealt here. The dark conductivity of the low C_H (10–15 at. %) films is approximately two orders of magnitude larger than the high C_H films, and the Fermi level distance from conduction band, determined by thermal activation analysis, is correspondingly smaller (~ 0.75 vs $\sim 0.9\text{ eV}$).²⁹ These values indicate that no significant band bending is present either at the film/substrate or film/air interfaces, since band bending would create a conductive “channel” and reduce the measured activation energies.

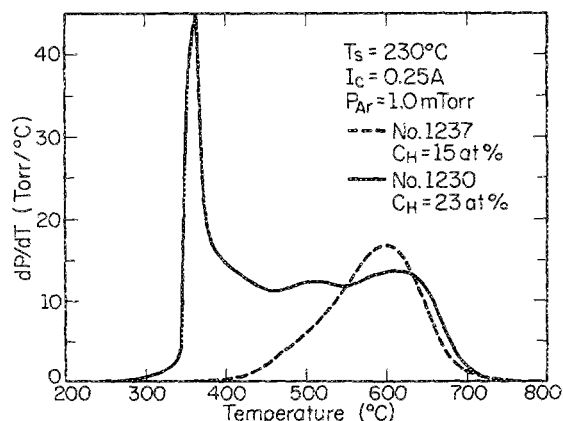


FIG. 3. The first derivative dP/dT hydrogen thermal evolution spectra for low and high C_H films. The spectra are normalized for 1 cm^2 *a*-Si:H film in a closed volume of 50 cc and the heating rate β was a constant $15^\circ\text{C min}^{-1}$.

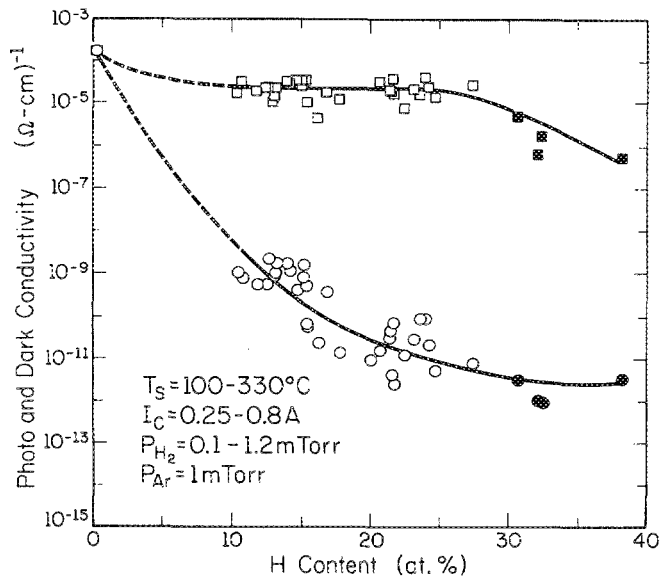


FIG. 4. Photo (AM-1) and dark conductivity as a function of the total C_H of the films for all the deposition conditions. We did not study the SWE on films having $C_H > 28$ at. % which were not high quality in the as-deposited state.

The photoconductivity (σ_{ph}) of the films diminishes with light exposure. The relative reduction in σ_{ph} [$\sigma_{ph}(t)/\sigma_{ph}(0)$] is shown as a function of C_H for 0.5, 3, and 15 h of red light exposure (150 mW/cm^2). All the films have $\sigma_{ph} = 0.9-3 \times 10^{-5} (\Omega \text{ cm})^{-1}$ in the initial state. The decrease from the annealed state is strongly dependent upon the exposure time (a few minutes induces $\sim 10\%$ drop on high hydrogen content films). To minimize errors at $t = 0$, the photoconductivities were first measured using 5 s of light exposure before the DOS measurements. All the light exposure studies in Fig. 5 were done with the same lamp and 150 mW/cm^2 light intensity.

The top curve in Fig. 5 shows the relative decrease in σ_{ph} after 30-min exposure as a function of C_H . The drop in σ_{ph} is $\sim 15\%-20\%$ for $C_H \sim 10\%-15\%$, and increases to $\sim 50\%$ for $C_H \geq 20\%$. This behavior, a larger reduction in photoconductivity for high C_H films, is emphasized after 3 and 15 h of light exposure. Note that the sharp reduction occurs at the same C_H (~ 15 at. %) where the films start to incorporate additional hydrogen in the 2100 cm^{-1} mode. With respect to the discussion in the previous section, the results in Fig. 5 suggest that there is a strong relation between light induced degradation and the hydrogen bonding and microstructure of the dc magnetron RS films.

Selected RS samples containing low and high hydrogen contents were light soaked to longer times. The film with low C_H was prepared at 0.2-mTorr hydrogen partial pressure and 300°C substrate temperature. We light soaked another low C_H film (13 at. %) for 15 h which had been deposited at 230°C and 0.2-mTorr hydrogen partial pressure. The behavior of these two films (both the decrease in σ_{ph} and the increase in DOS) were identical in this light exposure time range. The film with high C_H was prepared at 1-mTorr hydrogen partial pressure in argon and a 230°C substrate temperature. For all films the argon partial pressure was kept

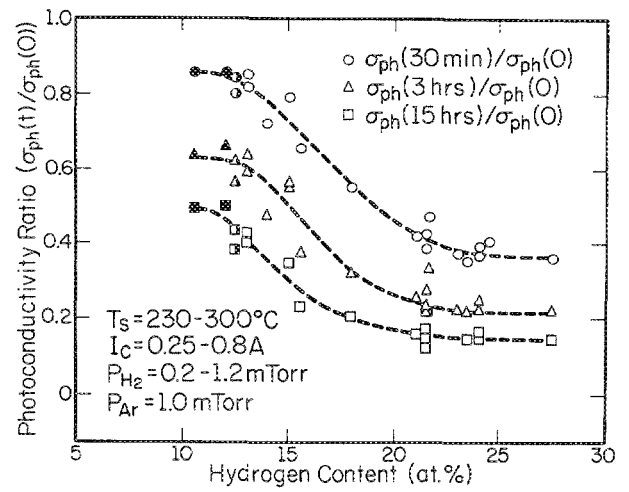


FIG. 5. The reduction in photoconductivity, [$\sigma_{ph}(t)/\sigma_{ph}(0)$], as a function of the total hydrogen content of the films. The degradation studies and σ_{ph} measurements are done under red light ($620-680 \text{ nm}$) with 150 mW/cm^2 . This figure shows a strong correlation between hydrogen content and reduction in σ_{ph} of the magnetron reactive sputtered $a\text{-Si:H}$. All samples have similar σ_{ph} (AM-1) in the as deposited state [$0.9-3 \times 10^{-5} (\Omega \text{ cm})^{-1}$]. The substrate temperature was kept constant at 230°C for all the films, except the filled and half filled data points which were measured on films deposited at 300 and 275°C , respectively: the hydrogen partial pressure during deposition was kept constant at 0.2 mTorr for these films.

constant at 1 mTorr . Figure 6 shows the reduction of σ_{ph} versus time and our measurement of the SWE on a device quality glow discharge produced $a\text{-Si:H}$ film with $C_H \sim 10$ at. %.⁴¹ This is similar to that observed by other groups.^{15,42} All three films have nearly the same σ_{ph} in the as-deposited state under 150 mW/cm^2 red light ($620-680 \text{ nm}$) illumination, but the rate of reduction in σ_{ph} is different. Both the glow discharge film and the high C_H reactively sputtered

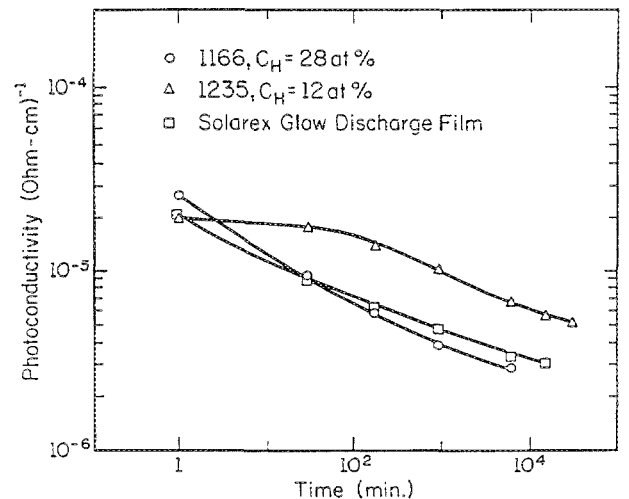


FIG. 6. The reduction in σ_{ph} as a function of the light exposure time for a low and a high C_H magnetron reactively sputtered and a glow discharge produced $a\text{-Si:H}$ film. All the films have similar σ_{ph} in the as deposited state, but the low C_H film has about a factor of two higher σ_{ph} after long light exposure compared to the others. The σ_{ph} measurements are done under 150 mW/cm^2 red light.

film degrade rapidly compared to the low C_H reactively sputtered film. After 100 h of light exposure, σ_{ph} for the low C_H film is ~ 3 times higher than σ_{ph} of the other two samples. Similar behavior has been observed on four other DC magnetron RS films with low and high C_H .

We did not observe a large decrease in dark conductivity of these films upon light exposure: the decrease was less than a factor of two for all the RS films. We also measured the dark conductivity activation energy of the low and the high C_H films after light exposure, using a temperature range of 30–140 °C to avoid annealing effects, and did not observe any significant changes. This indicates that the dark Fermi level does not move upon light exposure, in agreement with the very small decrease in room temperature dark conductivity.

C. Changes in the density of defect states

The DOS in the band gap of *a*-Si:H increases under light exposure and this degrades the carrier transport properties by reducing the carrier lifetimes. Figures 7(a) and 7(b)

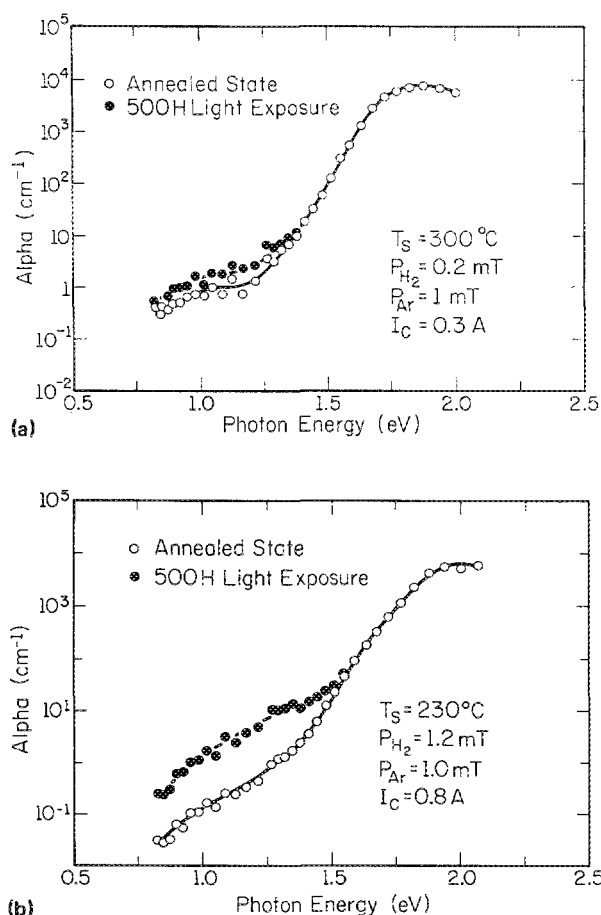


FIG. 7. (a) The CPM spectra for a low C_H film (12 at. %) in the as-deposited state (open circles) and after 500 h of light exposure (filled circles); there is a small increase in the optical absorption coefficient in the low photon energy (0.8–1.5 eV) region. (b) The CPM spectra for a high C_H film (22 at. %) in the as-deposited state (open circles) and after 500 h of light exposure (filled circles); the increase in the optical absorption coefficient in the low photon energy (0.8–1.5 eV) region is quite large.

show the normalized CPM subgap absorption spectra for low (12 at. %) and high C_H (22 at. %) films in the as-deposited state and after light exposure. The DOS is determined from the area at energies less than the exponential edge³⁹ using a constant of proportionality factor of $1.9 \times 10^{16} \text{ cm}^{-3}$.^{3,43} For the high C_H film there is approximately an order of magnitude increase in the optical absorption for photon energies less than ~ 1.4 eV. To measure the increase in the density of defect states as a function of light exposure time and C_H , the DOS was measured for a series of films in the annealed state and after 0.5, 3, and 15 h of light exposure.

The DOS in the annealed state and after 15 h of light exposure is shown in Fig. 8 as a function of total C_H of the films. (For clarity the DOS after 30 min and 3 h of exposure are not shown.) In the annealed state, low C_H (10–15 at. %) films have 3–5 times higher DOS than the high C_H (≥ 17 at. %) films. After 15 h of light exposure the DOS increases by an order of magnitude for high C_H films; at this stage they have a factor of two higher DOS than the low C_H films. If the quality of the material was simply judged from their properties in the as-deposited state, the high C_H films would be the best choice based on Figs. 4 and 8. However, the increase in DOS only after 15 h of light exposure shows that the quality of *a*-Si:H films in the as-deposited state cannot be taken alone to judge the electronic quality of the material.

The photoconductivity ($\sigma_{ph} = qG\mu\tau$ where q is the electronic charge, G is the electron-hole pair generation rate, μ and τ are electron mobility and recombination lifetime, respectively) does not scale as $\sigma_{ph} \propto 1/\text{DOS}$ (Ref. 44) between samples in the as-deposited state as seen from Figs.

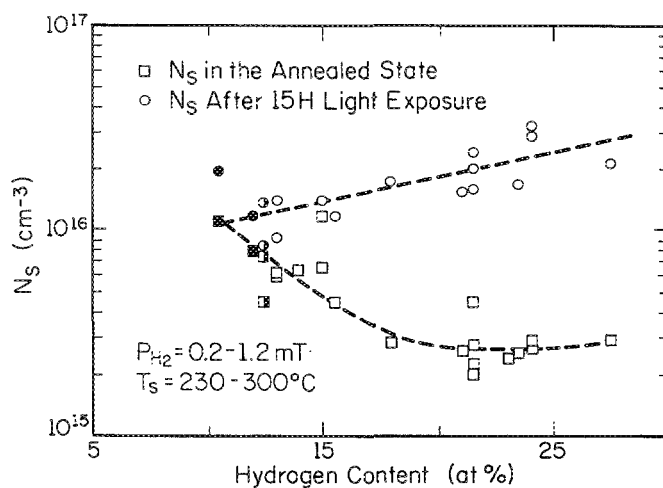


FIG. 8. The total density of defect states as a function of the total C_H for annealed films and after 15 h of light exposure. These results indicate that the quality of the material can not be simply judged from the initial properties. These results and those in Fig. 5 indicate that there is a fundamental correlation between the total C_H and the SWE of the *a*-Si:H films. The substrate temperature was kept constant at 230 °C for all the films, except the filled and half filled data points which were measured on films deposited at 300 and 275 °C, respectively; the hydrogen partial pressure during deposition was kept constant at 0.2 mTorr for these films.

4 and 8.^{29,30} The low C_H films have a higher generation rate (G) under AM-1 light due to their lower optical band gaps. When we normalize our σ_{ph} data in Fig. 4 to constant G , we find a factor of ~ 2 decrease in σ_{ph} as DOS increases by a factor of ~ 5 between samples.

The number of created defect states (ΔN_s) after 30 min and 15 h of light exposure as a function of total hydrogen content of the films is shown in Fig. 9. The ΔN_s increases almost exponentially as a function of total hydrogen content both after 30 min and 15 h of light exposure. These results suggest a fundamental relationship between Staebler-Wronski effect and the total C_H of the films. The number of newly created defect states after 15 h of light exposure are also shown as a function of the initial DOS in Fig. 10. ΔN_s after 15 h of light exposure is less for low C_H films, which have higher DOS in the as deposited state. These results differ with those reported in Refs. 17 and 18 in which the ΔN_s was higher for films with high initial DOS. However, the initial DOS in their films was as high as $\sim 2 \times 10^{17} \text{ cm}^{-3}$ (Ref. 18) and $8 \times 10^{18} \text{ cm}^{-3}$ (Ref. 17), which is outside the range for device quality material.

The increase in the DOS as a function of the light exposure time is shown in Fig. 11 for the same films reported in Fig. 6. As shown in the photoconductivity results, low C_H magnetron RS films are more stable against light induced degradation compared to high C_H magnetron RS and a device quality glow discharge produced film. The glow discharge produced film and high C_H reactive sputtered films have a factor of 3–5 times less DOS than the low C_H film in the as-deposited state; however after a few hours of light exposure the DOS for low C_H film becomes less than the other two films. Further light exposure increases the difference in the DOS between these films since the number of created defect states is less for low C_H films (Fig. 9). Similar long time behavior was observed on two other low C_H films with exposures up to 100 h and all low C_H films studied showed similar behavior for exposures up to 15 h as seen in Fig. 8.

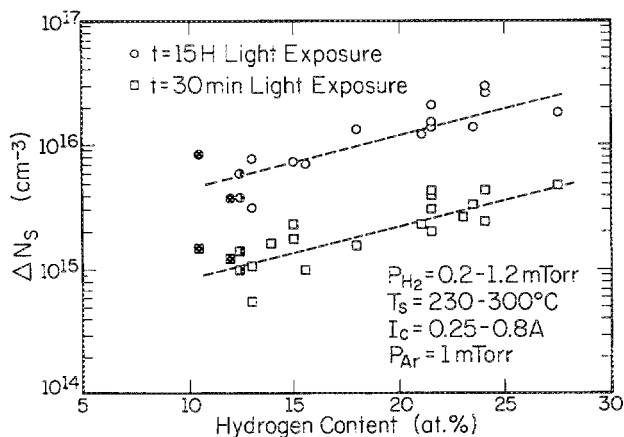


FIG. 9. The number of created defect states after 30 min and 15 h of light exposure as a function of the total hydrogen content. The substrate temperature was kept constant at 230 °C for all the films, except the filled and half filled data points which were measured on films deposited at 300 and 275 °C, respectively; the hydrogen partial pressure during deposition was kept constant at 0.2 mTorr for these films.

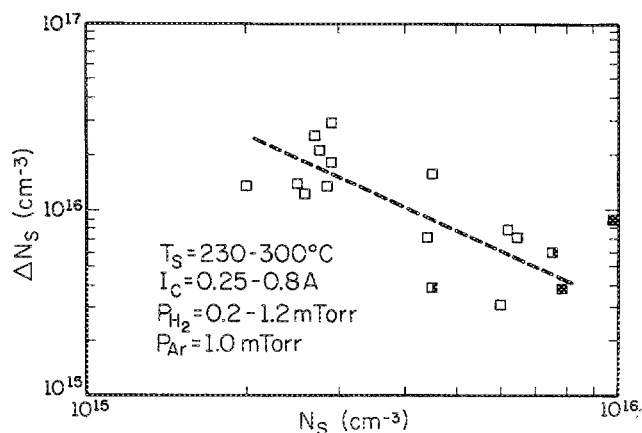


FIG. 10. The number of created defect states as a function of the initial defect states. The films that have lower initial defect states are more susceptible to the light induced degradation. The substrate temperature was kept constant at 230 °C for all the films, except the filled and half filled data points which were measured on films deposited at 300 and 275 °C, respectively; the hydrogen partial pressure during deposition was kept constant at 0.2 mTorr for these films.

A more quantitative measure of light exposure is the total number of photons absorbed by the material. In the spectral range used here, the low C_H films have \sim twofold higher generation rate than the high C_H films due to their smaller optical band gaps, i.e., they have larger optical absorption coefficients. Figure 12 shows the increase in DOS as a function of the number of photons absorbed (generation

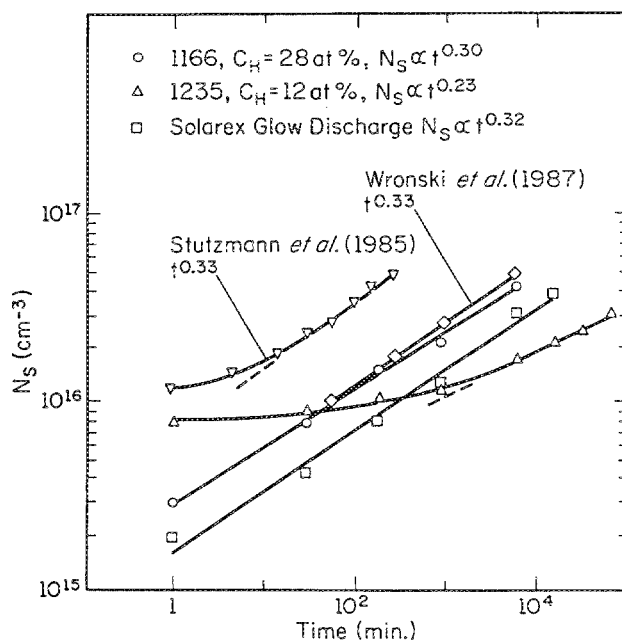


FIG. 11. The DOS (measured by CPM) as a function of the light exposure time at $I = 150 \text{ mW/cm}^2$ for two representative dc magnetron reactive sputtered films and a glow discharge produced film. The low C_H film is superior against SWE compared to the high C_H and glow discharge produced films. The SWE results of Stutzmann *et al.* ($I = 200 \text{ mW/cm}^2$, ESR),¹⁵ and Wronski *et al.* ($I = 50 \text{ mW/cm}^2$, CPM data)⁷ for GD produced films are also shown for comparison. Light intensity does not effect the slope of the curves.

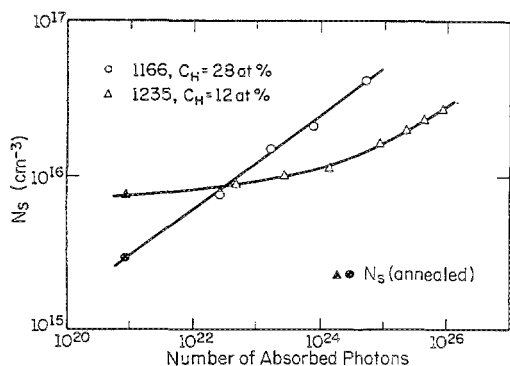


FIG. 12. The DOS as a function of the number of absorbed photons (generation rate \times exposure time) during light exposure. Compared to Fig. 11 the crossover in DOS for dc magnetron reactively sputtered films occurs earlier in the light exposure.

rate \times exposure time). When quantified in this fashion, the crossover (Fig. 11) occurs even earlier in the exposure.

D. Discussion

In this section we compare our results with the predictions of Stutzmann's band to band recombination model.¹⁵ First, the model predicts that at long times the defect state concentration should increase as $t^{1/3}$. In Fig. 11 our results for the low C_H film, indicate a $t^{0.23}$ dependence of the DOS on exposure time between 100 and 1000 h (the longest time examined). The slope is determined from last four data points. It is possible that the RS films will take on the $t^{1/3}$ dependence with longer exposure, however our results do not indicate a significant evolution in slopes. If we assume that we will eventually observe the $t^{1/3}$ rule, we do not see a good fit between the measured and the calculated data. In addition the susceptibility coefficient, A_{s-w} [Eq. (1)], would be approximately $100\times$ less for films with a low C_H compared to high C_H , which indicates that the low C_H films are far better against SWE. The fit with data is good if we take the time dependence as $t^{0.23}$, but this cannot be rationalized within the theory.

Identical measurements were performed on a glow discharge produced film. As shown in Fig. 11, $\sim t^{1/3}$ behavior is observed for this sample in accordance with the results reported by other groups.^{7,15,42} The magnetron RS films with high C_H degrade a little slower than the glow discharge produced films, but much faster than the low C_H films.

Second, the band to band model does not predict a crossover for the DOS curves. The crossover in Fig. 11 is a clear indication that the defect creation kinetics must be fundamentally different for low C_H films. In Stutzmann's model, the initial DOS affects the initial rate of defect creation by a shunting mechanism. Recombination events proceed either through band tails, which create defects with a probability A_{s-w} , or through mid-gap states which dissipate the pair energy without defect creation. A large initial DOS will dominate the recombination traffic and reduce the defect formation rate. However, if the recombination pathways and the A_{s-w} coefficients are identical in two films with different initial DOS values, then they must asymptotically approach

the same DOS vs t behavior at long times. The low C_H magnetron RS film has a lower DOS for long times. We note then that the initial DOS is not a reliable indicator of α -Si:H quality in terms of stability.

A final point concerns the photoconductivity exponents γ and δ (where $\sigma_{ph} \propto G^\gamma N_s^{-\delta}$) which give information on the recombination mechanism for excess carriers. Stutzmann *et al.*¹⁵ measured γ and δ for glow-discharge produced films, found them close to unity, and derived their model based on $\gamma = \delta = 1$. We find that γ and δ depend on the total C_H of the magnetron RS films as listed in Table II. γ increases nearly linearly from ~ 0.73 to ~ 0.95 as C_H increases from 10 to 28 at. % as shown in Fig. 13.³² The photoconductivity of the films as a function of the density of defect states is shown in Fig. 14; this includes films which have been exposed to light for 100 h or more. The low C_H films have systematically higher δ values compared to the high C_H films. $\delta = 0.85$ for C_H of 21–28 at. % is comparable to the value obtained by Stutzmann *et al.* for dc photoconductivity in their GD films. We measured a δ value of 0.62 for a GD produced film⁴¹ which agrees with the results reported by Shepard *et al.*⁴⁵ for a similar range of generation rates. Those authors modified the Stutzmann model in an attempt to account for measured δ differences between GD films. However, the modified model does not agree well with our results for RS films.

E. How does hydrogen content control the SWE of α -Si:H?

We have suggested that the total C_H of our magnetron RS α -Si:H films controls the hydrogen bonding, microstructure, optical and electronic properties in the as deposited state; here we make a similar assertion for the light induced degradation behavior. Recall that there are two stages for the creation of dangling silicon bonds in microscopic model (Fig. 1). The first stage is the breaking of weak Si—Si bonds. The second stage is the isolation of these newly broken bonds by hydrogen motion before they recombine.

The breaking of weak silicon—silicon bonds is believed to be driven by the energy released from free carrier band-to-band recombination events. The probability for this process is thought to increase with the pair energy, i.e., the band gap. We reported a linear increase in the optical band gap (Tauc gap) of ~ 0.0125 eV/at. % H as the C_H of our RS films increases.^{29,32} This implies that the average energy released per band to band recombination increases ~ 0.2 eV from low

TABLE II. Shows the γ and δ values for selected magnetron RS films with varying hydrogen content and the total light exposure time. The γ values are measured after 30 min of light exposure.

Sample No.	C_H (at. %)	γ	δ	Length of light exposure (h)
1166	28	0.93	0.85	100
1232	21	0.88	0.84	100
1235	12	0.78	1.23	1000
1240	11	0.75	1.23	100

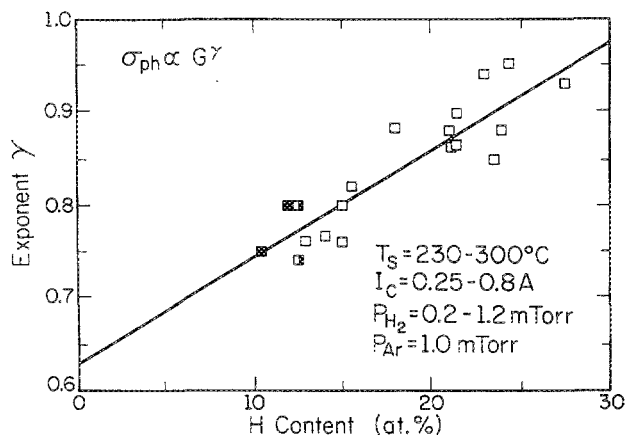


FIG. 13. The increase in photoconductivity exponent γ ($\sigma_{ph} \propto G^\gamma$) as a function of C_H . The substrate temperature was kept constant at 230 °C for all the films, except the filled and half filled data points which were measured on films deposited at 300 and 275 °C, respectively: the hydrogen partial pressure during deposition was kept constant at 0.2 mTorr for these films.

to high C_H films. The weak Si—Si bonds are therefore more likely to be broken in high C_H films due to the higher optical band gap. This observation is in agreement with data published by Skumanich and Amer⁴⁶ for amorphous alloy materials with varying optical band gaps, and the results obtained by Kolodzey *et al.*⁴⁷ for low band gap (> 1.4 eV) a -Si:Ge:H alloys which show a low rate of degradation.

Smith and Wagner⁴⁸ postulated that highly strained Si—Si bonds have electron states in the valence band tail, and are those which convert to dangling bonds upon light exposure. The density of these strained states can be inferred from the exponential portion of the optical absorption edge (the Urbach slope, E_0) because the valence band tail dominates this slope. We have observed a 7–8 meV increase in

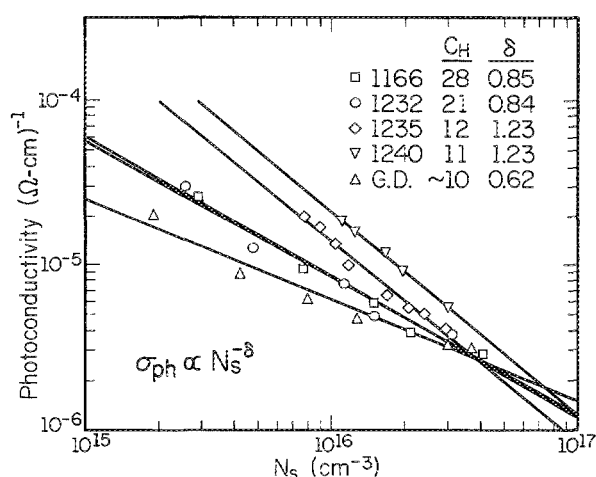


FIG. 14. The change in photoconductivity (σ_{ph}) as a function of the density of defect states ($\sigma_{ph} \propto N_s^{-\delta}$) during light soaking for low and high C_H RS films and a GD produced film. Films with low C_H have higher δ values (also see Table II). The σ_{ph} measurements are done under 150 mW/cm² red light. The solid lines are least squares fit to the data.

Urbach slope for some films from photoconductivity sub gap absorption measurements as the hydrogen content of the films increased.³² From CPM measurements we did not see a clear correlation between the Urbach slope ($E_0 \sim 50$ meV) and the hydrogen content of the films indicating that there is no clear relationship between the C_H and the density of strained Si—Si bonds in magnetron RS films.

The second stage of the degradation process involves the isolation of the newly created broken bonds before they reform. The isolation may occur by the exchange of neighboring hydrogen and dangling bond sites as shown in Fig. 1. The stabilization process may be favored in high C_H material. We reported that as C_H increases above 15 at. %, the additional H goes into dihydride modes and the microstructure becomes void rich.^{30,31} Both aspects have been associated with increased susceptibility to degradation. As discussed earlier Carlson's model involves the motion of hydrogen in the internal surfaces of microvoids and proposes that increasing the density (lowering the void content) should increase the stability of a -Si:H.²⁰ Bhattacharya and Mahan²¹ reported that material with greater SiH₂ content (which they associate with void density) is more susceptible to light induced defect creation. Kakalios *et al.*⁴⁹ associate the motion of hydrogen with the annealing of the defect states in a -Si:H which indicates that hydrogen is involved in the degradation process. Our results are in agreement with these assertions.

Increasing the total C_H of the films not only reduces the density of defect states, but also changes the defect state distribution in the band gap. Low C_H films have lower γ and higher δ (Figs. 13 and 14). In general, a change in γ or δ indicates a shift in the dominant recombination pathway. If this change reduces the band to band recombination rate, it will suppress the SWE for the film.

The experimental data presented here show that increasing the hydrogen content of a -Si:H films increases the susceptibility to light induced degradation. We propose that this takes place by enhancing both stages of the degradation mechanism shown in Fig. 1. These effects are to increase the probability of breaking weak silicon—silicon bonds by raising the band gap and to increase the efficiency of isolating these broken silicon bonds, perhaps on microvoid surfaces. Our results are also in accordance with the predictions of Carlson's model.²⁰

IV. CONCLUSIONS

We have evaluated the susceptibility of magnetron reactively sputtered a -Si:H to light induced degradation and identified a relationship between the total hydrogen content and the Staebler–Wronski effect. This effect has been a potential limitation in the use of a -Si:H for long term applications such as photovoltaic devices. The total hydrogen content of the films was independently controlled by the hydrogen partial pressure in the sputtering plasma during deposition, which is an independent variable not available in plasma assisted chemical vapor deposition methods. In the as-deposited state, sputtered films with low C_H (10–15 at. %) have higher initial defect densities, but are superior against light induced degradation, compared to a high C_H

(≥ 17 at. %) or a typical glow discharge produced film. The DOS increases as $t^{0.23}$, $t^{0.3}$, and $t^{0.33}$ for low (12 at. %) and high hydrogen content (28 at. %) magnetron reactive sputtered films, and the glow discharge film, respectively.

This study also showed that Stutzmann's band to band recombination model¹⁵ predicts the behavior of a glow discharge produced *a*-Si:H film but does not agree with our results for the highly stable low C_H magnetron reactively sputtered *a*-Si:H films. Our data agree with the two stage microscopic degradation mechanism proposed by Dersch *et al.*³

ACKNOWLEDGMENTS

Professor John A. Thornton, who originated this research project, passed away unexpectedly in November 1987. We are indebted to his guidance and dedicate our work to him. We would like to thank Dr. Nagi Maley for measuring the hydrogen content and Dr. Charles Fortman (Solarex Corporation) for supplying the glow discharge deposited *a*-Si:H film. We also would like to thank Professor Christopher Wronski from Pennsylvania State University and Professor Sigurd Wagner from Princeton University for many inspiring discussions. This work was supported by the Electric Power Research Institute.

- ¹ D. L. Staebler, and C. R. Wronski, *Appl. Phys. Lett.* **39**, 292 (1977).
- ² I. Hirabayashi, K. Morigaki, and S. Nitta, *Jpn. J. Appl. Phys.* **19**, L357 (1980).
- ³ H. Dersch, J. Stuke, and J. Beichler, *Appl. Phys. Lett.* **38**, 456 (1981).
- ⁴ D. V. Lang, J. D. Cohen, J. P. Harbison, and A. M. Sergent, *Appl. Phys. Lett.* **40**, 474 (1982).
- ⁵ J. I. Pankove and J. E. Berkeyheiser, *Appl. Phys. Lett.* **37**, 705 (1980).
- ⁶ A. Skumanich and N. M. Amer, *Appl. Phys. Lett.* **52**, 643 (1985).
- ⁷ C. R. Wronski, Z. E. Smith, S. Aljishi, V. Chu, K. Shepard, D. S. Shen, R. Schwarz, D. Slobodin, and S. Wagner, *AIP Conf. Proc.* **157**, 70 (1987).
- ⁸ C. R. Wronski, *AIP Conf. Proc.* **157**, 1 (1987).
- ⁹ D. L. Staebler and C. R. Wronski, *J. Appl. Phys.* **51**, 3262 (1980).
- ¹⁰ D. L. Staebler, R. S. Crandall, and R. Williams, *Appl. Phys. Lett.* **39**, 733 (1981).
- ¹¹ S. Guha, J. Yang, W. Gzubytyj, S. J. Hudgens, and M. Hack, *Appl. Phys. Lett.* **42**, 589 (1983).
- ¹² I. Sakata, Y. Hayashi, H. Karasawa, and M. Yamanaka, *Solid State Commun.* **45**, 1055 (1984).
- ¹³ H. Pfeleiderer, W. Kusian, and W. Kruhler, *Solid State Commun.* **49**, 493 (1984).
- ¹⁴ W. Kruhler, H. Pfeleiderer, R. Plattner, and W. Stetter, *AIP Conf. Proc.* **120**, 311 (1984).
- ¹⁵ M. Stutzman, W. B. Jackson, and C. C. Tsai, *Phys. Rev. B* **32**, 23 (1985).
- ¹⁶ R. A. Street, D. K. Biegelsen, and J. C. Knights, *Phys. Rev. B* **24**, 363 (1981).
- ¹⁷ T. Shimizu, M. Kumeda, A. Morimoto, H. Yokomichi, and N. Ishii, *J. Non-Cryst. Solids* **77-78**, 377 (1985).
- ¹⁸ M. Ohsawa, T. Hama, T. Akasaka, T. Ichimura, H. Sakai, S. Ishida, and Y. Uchida, *Jpn. J. Appl. Phys.* **24**, L838 (1985).
- ¹⁹ S. Nakano, H. Tarui, H. Haku, T. Takahama, T. Matsuyama, M. Iso-mura, M. Nishikuni, N. Nakamura, S. Tsuda, M. Ohnishi, and Y.

- Kuwano, in *Proceedings of the 19th IEEE Photovoltaics Specialist Conference*, (IEEE, New York, 1987), p. 678.
- ²⁰ D. E. Carlson, *Appl. Phys. A* **41**, 305 (1986).
- ²¹ E. Bhattacharya and A. H. Mahan, *Appl. Phys. Lett.* **52**, 1587 (1988).
- ²² D. A. Anderson, T. D. Moustakas, and W. Paul, in *Amorphous and Liquid Semiconductors*, edited by W. E. Spear (University of Edingburgh, Scotland, 1977), p. 334.
- ²³ T. D. Moustakas and W. Paul, *Phys. Rev. B* **15**, 1564 (1977).
- ²⁴ D. A. Anderson and W. Paul, *Philos. Mag. B* **44** (2), 187 (1981)
- ²⁵ T. D. Moustakas, in *Hydrogenated Amorphous Silicon, Semiconductors and Semimetals*, edited by J. I. Pankove (Academic, New York, 1984), Vol. 21-A, p. 55.
- ²⁶ M. J. Thompson, in *The Physics of Hydrogenated Amorphous Silicon I*, edited by J. D. Joannopoulos and G. Lucovsky (Springer, New York, 1984), Vol. 55, p. 119.
- ²⁷ N. Sayvides, *J. Appl. Phys.* **56**, 2788 (1984)
- ²⁸ H. Rubel, B. Schroder, and J. Geiger, *J. Vac. Sci. Technol. A* **4**, 1855 (1986).
- ²⁹ M. Pinarbasi, N. Maley, M. J. Kushner, A. Myers, J. R. Abelson, and J. A. Thornton, *J. Vac. Sci. Technol.* **7**, 1210 (1989).
- ³⁰ M. Pinarbasi, N. Maley, N., A. Myers, and J. R. Abelson, *Thin Solid Films* **171**, 217 (1989).
- ³¹ M. Pinarbasi, N. Maley, A. Myers, I. Szafrank, J. R. Abelson, and J. A. Thornton, *Amorphous Silicon Technology*, edited by A. Madan, M. J. Thompson, P. C. Taylor, P. G. LeComber, and Y. Hamakawa (MRS, Pittsburgh, 1988), Vol. 118, p. 537.
- ³² M. Pinarbasi, Ph.D. Thesis, University of Illinois at Urbana-Champaign (1989).
- ³³ M. Hicks, S. Lee, S. Kumar, C. R. Wronski, and M. Pinarbasi, *Amorphous Silicon Technology*, edited by A. Madan, M. J. Thompson, P. C. Taylor, Y. Hamakawa, and P. G. LeComber (MRS, Pittsburgh, 1989), Vol. 149, p. 303.
- ³⁴ M. Pinarbasi, N. Maley, J. R. Abelson, V. Chu, and S. Wagner, *Amorphous Silicon Technology*, edited by A. Madan, M. J. Thompson, P. C. Taylor, Y. Hamakawa, and P. G. LeComber (MRS, Pittsburgh, 1989), Vol. 149, p. 205.
- ³⁵ M. Pinarbasi, M. J. Kushner, and J. R. Abelson, *Appl. Phys. Lett.* **56**, 1685 (1990).
- ³⁶ M. Pinarbasi, L. H. Chou, N. Maley, A. Myers, D. Leet, and J. A. Thornton, *Superlattices and Microstructures* **3**, 331 (1987).
- ³⁷ J. A. Thornton, *J. Vac. Sci. Technol.* **11**, 666 (1974).
- ³⁸ J. A. Thornton, in *Amorphous Metals and Semiconductors*, Vol. 3 *Acta Scripta Metallurgica Series*, edited by P. Haasen and R. I. Jaffee (Pergamon, Oxford, 1986), p. 229.
- ³⁹ M. Vanacek, J. Kocka, J. Stuchiik, Z. Kozisek, O. Stika, and A. Triska, *Solar Energy Materials* **8**, 41 (1983).
- ⁴⁰ N. Maley, A. Myers, M. Pinarbasi, D. M. Leet, J. R. Abelson, and J. A. Thornton, *J. Vac. Sci. Technol.* **7**, 1210 (1989).
- ⁴¹ Glow discharge sample and its hydrogen content estimation is provided by Dr. Charles Fortman of Solarex Corporation.
- ⁴² A. G. Kazanskii, E. P. Milichevich, and V. S. Vaslov, *J. Non-Cryst. Solids*, **97&98**, 787 (1987).
- ⁴³ Z. E. Smith, V. Chu, K. Shepard, S. Aljishi, D. Slobodin, J. Kolodzey, and S. Wagner, *Appl. Phys. Lett.* **50**, 1521 (1987).
- ⁴⁴ A. Rose, *Concepts in Photoconductivity and Allied Problems* (Interscience, New York, 1963).
- ⁴⁵ K. Shepard, Z. E. Smith, S. Aljishi, and S. Wagner, *Amorphous Silicon Technology*, edited by A. Madan, M. J. Thompson, P. C. Taylor, P. G. LeComber, and Y. Hamakawa (MRS, Pittsburgh, 1988), Vol. 118, p. 147.
- ⁴⁶ A. Skumanich and N. M. Amer, *Appl. Phys. Lett.* **52**, 643. (1988).
- ⁴⁷ J. Kolodzey, R. Schwarz, S. Aljishi, V. Chu, D. S. Shen, P. M. Fauchet, and S. Wagner, *Appl. Phys. Lett.* **52**, 477 (1988).
- ⁴⁸ Z. E. Smith, S. Wagner, in *Advances in Amorphous Semiconductors* edited by H. Fritzsche (World Scientific, Singapore, 1988), p. 67.
- ⁴⁹ J. Kakalios, R. A. Street, and W. B. Jackson, *Phys. Rev. Lett.* **59**, 1037 (1987).